文章编号:1001 - 2060(2016)11 - 0069 - 05

六回路循环流化床锅炉单回路中断的影响实验研究

邹阳军[1],程乐鸣[2],何　胜[1]
(1. 华电电力科学研究院,浙江 杭州 310030; 2. 浙江大学 能源清洁利用国家重点实验室,浙江 杭州 310027)

摘　要: 在六回路(6 个物料外循环回路) 超临界 CFB(循环流化床) 锅炉冷态实验台上,采用差压法测定炉内颗粒浓度分布,研究单回路中断受阻时炉内颗粒浓度的变化规律及不同回路中断受阻时对炉内颗粒浓度变化规律。结果表明: 单回路中断受阻后,炉内轴向平均颗粒浓度成指数型下降,恢复回路正常回料后,系统重新恢复到初始平衡状态,说明"双支腿"型 CFB 锅炉具有自平衡特性。单回路中断受阻后,炉内横向截面各区域颗粒浓度分布仍较为均匀; 不同的单回路中断受阻时,炉内中上部区域颗粒浓度变化规律无明显差异,密相区变化规律则较为复杂。

关　键　词:六回路; 循环流化床; 颗粒浓度; 单回路中断受阻

中图分类号:TK229.2　　**文献标识码**:A

DOI:10.16146/j.cnki.rndlgc.2016.11.013

引　言

在 CFB 锅炉发展的早期,由于锅炉容量较小,炉内物料浓度及温度分布不均问题并不突出,而随着 CFB 锅炉朝着超临界方向发展,床层截面不断增大,炉内物料分布不均匀的问题也越发受到重视[1~2]。对于采用"双支腿"结构的 CFB 锅炉而言,当容量放大到 600 MW 超临界时,为保持二次风的穿透性,炉膛尺寸在深度方向变化不大,而主要在宽度方向进行放大,从而使得宽深比明显增大。宽深比的增大,必然导致物料沿炉膛截面宽度方向扩散更加困难。如果返料和新加入物料不能快速扩散均匀,会出现局部区域燃料堆积,偏置燃烧,料腿燃烧或尾部受热面积灰复燃等一系列问题[3~4],进而导致锅炉燃烧效率降低,甚至影响锅炉的安全稳定运行。因此,针对六回路超临界 CFB 锅炉循环回路回料失衡后,研究炉内颗粒浓度分布的变化规律有着重要的意义。

目前,针对 CFB 锅炉炉内颗粒浓度分布和循环流率的研究有很多[5~8],但关于循环回路回料中断受阻对炉内颗粒浓度分布的影响少有文献报道。本研究在一台六回路 600 MW 超临界 CFB 锅炉模化冷态实验台上,通过调节外置式换热器锥形阀和回料器回料风来模拟回路中断受阻,进而研究单回路回料中断受阻时,炉内颗粒浓度的变化规律及不同回路中断受阻对炉内颗粒浓度变化规律的影响。

1　实验装置及方法

近些年来,国内外学者开展了一系列的流化床冷态模化试验,其研究成果证明了选取合理的相似法则,从而建立小型模型实验台来模拟实际运行状况的方法是可行并且有效的。本研究选用欧拉双流体模型,并根据文献[9]中的模化计算方法,确定流化床模化准则数组为: $\frac{u_0^2}{gD}$, $\frac{\rho_f}{\rho_s}$, $\frac{u_0}{u_{mf}}$, $\frac{G_s}{\rho_s u_0}$, ϕ,床体几何结构,PSD(颗粒相对于其平均粒径的无因此粒径分布) u_0—风速,m/s; g—重力加速度,m/s^2; D—特征长度,m; ρ_f—空气密度,kg/m^3; ρ_s—床料密度,kg/m^3; u_{mf}—临界流化速度,m/s; G_s—固相流率,kg/m^3·s; ϕ—球形度; t—时间,s; x—长度,m。根据确定的模化准则数组,对东方锅炉 600 MW CFB 锅炉冷态实验台进行模化计算,步骤如下:

(1) 根据 $\frac{\rho_f}{\rho_s}$ 相等,选定流化介质,确定模型颗粒密度; (2) 选择几何比例,床内结构尺寸严格按几何比例,床外结构可以调整; (3) 根据 Fr 弗劳德数 $\frac{u_0^2}{gD}$ 相等, $\frac{(u_0)_m}{(u_0)_c} = \left(\frac{D_m}{D_c}\right)^{\frac{1}{2}}$,c—原型流化床锅炉; m—模型流化床锅炉,确定了模型床风速; (4) 根据 $\frac{u_0}{u_{mf}}$ 相等,得到

收稿日期: 2016 - 01 - 11; 修订日期: 2016 - 01 - 21

作者简介: 邹阳军(1988 -),男,江西上饶人,华电电力科学研究院火电技术研究所研究员.

模型颗粒临界流化速度，进而确定了床料粒径和分布；(5) 根据 $\frac{G_s}{\rho_s u_0}$ 相等，$\left(\frac{G_s}{\rho_s}\right)_m / \left(\frac{G_s}{\rho_s}\right)_c = \frac{(u_0)_m}{(u_0)_c} = \left(\frac{D_m}{D_c}\right)^{\frac{1}{2}}$，确定了单位面积固相流率；(6) 推论:时间比例 $\frac{t_m}{t_c} = \frac{\left(\frac{x_m}{u_m}\right)}{\left(\frac{x_c}{u_c}\right)} = \frac{\left(\frac{x_m}{x_c}\right)}{\left(\frac{u_m}{u_c}\right)} = \frac{\left(\frac{x_m}{x_c}\right)}{\left(\frac{x_m}{x_c}\right)^{\frac{1}{2}}} = \left(\frac{x_m}{x_c}\right)^{\frac{1}{2}}$。

根据模化计算，模化实验台各方向尺寸全部采用 1∶40 的尺寸比例，表 1 所示为模化计算的结果。

表 1 东方锅炉 600 MW CFB 锅炉冷态模化计算

Tab. 1 Cold-state modeling calculation of a 600 MW CFB boiler made by Dongfang Boiler Works

设计参数	实炉	模化实验台
高度 H/m	55.00	1.38
炉膛宽度 W/m	27.90	0.7
深度 D_c/m	15.03	0.375
床料	煤粉	玻璃粉
床料密度 ρ_s/kg·m^{-3}	2 000	2 300
床料粒径 d_p/μm	400	95
球形度 Φ	0.8	0.8
运行温度 T/℃	900	25
风速 u_0/m·s^{-1}	5.400	0.853 8
空气密度 ρ_f/kg·m^{-3}	0.301	1.225
运动粘度 ν/m^2·s^{-1}	1.55E-04	2.192E-05
动力粘度 μ/Pa·s	4.67E-05	1.96E-05
固相流率 G_s/kg·(m^2·s)$^{-1}$	16.56	3.01
临界流化速度 u_{mf}/m·s^{-1}	0.050	0.008
时间 t/s	1.00	0.158
u_0^2/gL	0.054	0.054
ρ_s/ρ_f	6 645	2 104
u_0/u_{mf}	107	107
$G_s/\rho_s u_0$	1.53E-03	1.53E-03

实验台主体由炉膛、6 只旋风分离器、6 只回料器和 6 只外置式换热器构成，并构成 6 个物料外循环回路，整体结构示意图如图 1 所示。实验台高 1.38 m，炉膛截面尺寸为 0.375 m×0.7 m。6 只旋风分离器分列炉膛两侧，成中心对称布置。炉膛底部采用“双支腿”结构设计，炉内设置有中隔墙，将炉膛上部一分为二。“双支腿”两侧布风板相对独立，由开孔的有机玻璃构成，通过控制布风板开孔率，覆盖滤布的方式使得布风板具有适当的阻力，以达到均匀布风的目的。实验台主体由有机玻璃构成，以便于观察炉内气固流动状态。

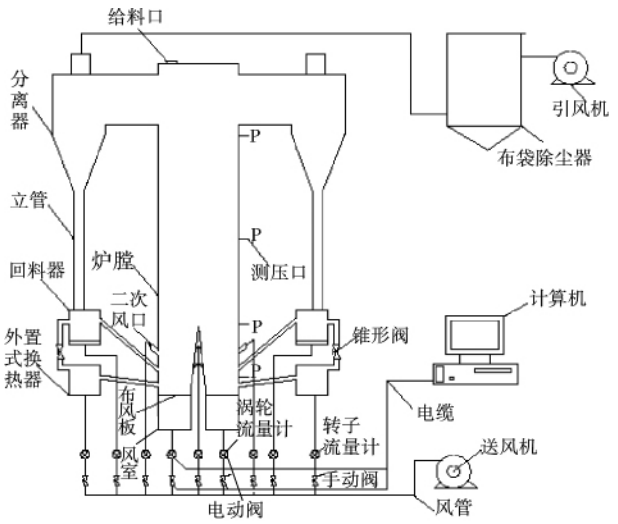

图 1 模型试验台系统图

Fig. 1 Systematic diagram of a model test rig

实验台控制测量系统由差压变送器、数据采集仪、异步电动机和计算机构成。差压变送器用以测量炉膛两侧墙上纵向测点间压差(两侧墙上压力测点布置方式如图 2 所示)，并采用差压浓度法公式 $\rho_P = \Delta P/(g\Delta h)$ 计算得到颗粒浓度分布，其中：ρ_P 为颗粒浓度，kg/m^3；ΔP 为纵向两测点间压差，Pa；g 为重力加速度，m/s^2；Δh 为纵向两侧点间高度差，m。

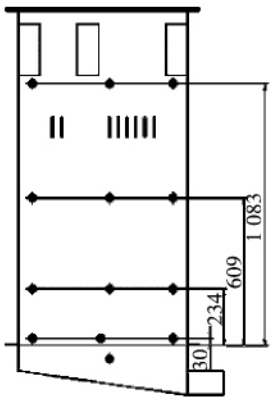

图 2 炉膛两侧墙压力测点布置图(mm)

Fig. 2 Chart showing the arrangement of the pressure measuring points(mm)

为方便讨论，将实验台 6 条外循环回路分别进行编号为 LA – LC 和 RA – RC，如图 3 所示，同时将炉膛轴向对应各回路划分为 ALA、ALB、ALC、ARA，ARB 和 ARC 共 6 个区域，由布置在各区域的差压变送器和数据采集仪测量记录压差，并计算得到各区域的轴向颗粒浓度实时变化。实验运行工况安排如表 2 所示。

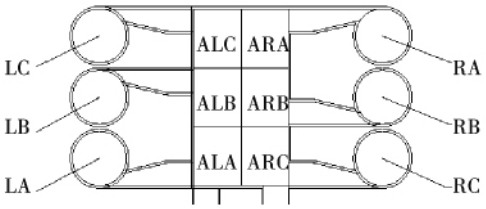

图 3　循环回路编号图

Fig. 3 Chart showing the serial numbers of circulating loops

表 2　实验运行工况设计

Tab. 2 Design of the operating conditions tested

运行参数	数值
空截面气速 u_0 /m · s^{-1}	0.75 ~ 1.06
静止床高 H_0 /mm	60、80
二次风比 λ /%	50
试验台运行温度/℃	50

2　试验结果分析

2.1　单回路中断受阻对炉内平均颗粒浓度的影响

CFB 锅炉炉内颗粒浓度分布直接影响炉内燃烧、传热、产物生产及磨损等，图 4 给出了装置稳定运行后，LB 回路中断受阻一段时间后，重新恢复回料，炉内各高度平均颗粒浓度的实时变化情况。

由图 4 可知，系统稳定运行时，炉内各高度颗粒浓度保持稳定。于 t = 250 s 关闭 LB 回路后，炉内各高度颗粒浓度逐渐下降，其原因在于物料在受阻回路中堆积，导致炉内物料量减少。恢复 LB 回路回料后，堆积的物料快速返回到炉膛，此时炉膛两侧回料不均，系统仍快速恢复到初始平衡状态。

图 5 给出了单回路部分受阻时，过渡区（h/H = 0.302）颗粒浓度随受阻时间 t_a 的变化图。随着 t_a 增加，受阻回路返料立管中物料堆积高度增加，受阻回路的回料速度增大，最终，受阻回路分离器进口物料量与回料量达到平衡，立管中物料高度保持稳定，系统再次处于动态平衡状态。由图 5 可知，此次试验平衡所需时间大约为 600 s，颗粒浓度随时间成指数型下降。

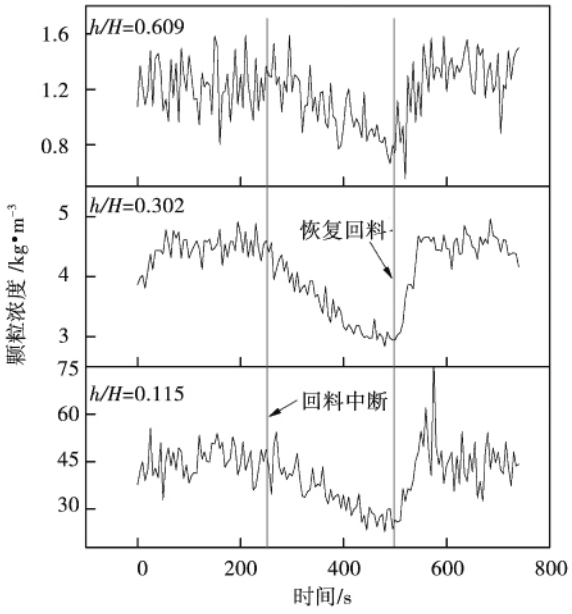

图 4　单回路中断 – 打开炉内各高度颗粒浓度变化图

Fig. 4 Chart showing changes of particle concentration in the furnace during the interruption – opening of a single loop at various heights

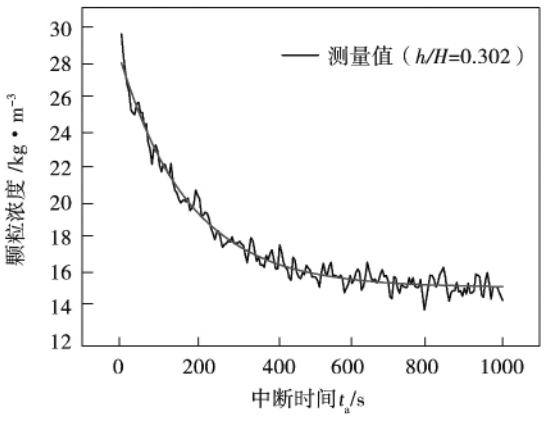

图 5　LB 回路受阻时 ALB（h/H = 0.302）颗粒浓度变化图

Fig. 5 Chart showing changes of the particle concentration（ALB – h/H = 0.302） when the loop LB is being blocked

2.2 单回路中断受阻对横向颗粒浓度分布的影响

图 6 给出了 LB 回路部分受阻后，过渡区（$h/H=0.302$）横向截面各区域颗粒浓度随受阻时间 t_a 的变化曲线。由图 6 可知，受阻回路 LB 所对应区域 ALB 与横向截面其它 5 个区域的颗粒浓度变化曲线无明显差异，中隔墙两侧颗粒浓度分布较为均匀，且变化趋势基本一致，其原因在于：单回路中断受阻后，因需要跨越中隔墙转移的物料量较少，中隔墙对两侧间物料转移的阻碍作用不明显，且物料在炉膛密相区横向扩散较为迅速，从而使得炉膛横向截面各区域颗粒浓度分布趋于一致，系统仍能维持稳定运行。

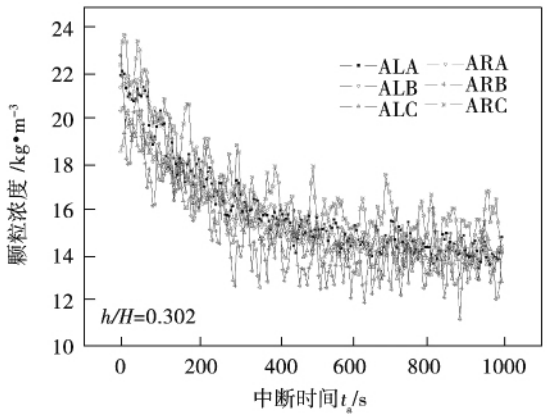

图 6 LB 回路中断受阻各区域（$h/H=0.302$）颗粒浓度变化图

Fig. 6 Chart showing changes of the particle concentration（$h/H=0.302$） in various zones when the loop LB is being interrupted and blocked

2.3 不同回路中断受阻的影响

研究表明，六分离器 CFB 锅炉同侧 3 个分离器外循环流率存在差异，中间分离器的循环流率低于两边的分离器[10]。由于实验台中 6 只分离器在炉膛两侧成中心对称分布，本文主要研究同侧不同回路中断受阻对炉内颗粒浓度的分布及变化规律的影响。待装置运行稳定后，分别使 RA、RB、RC 回路中断受阻，测量记录各高度 ALB 区域颗粒浓度随受阻时间 t_a 的变化，结果如图 7 ~ 图 9 所示。

图 7 和图 8 分别给出了炉膛上部稀相区和过渡区的颗粒浓度变化曲线。由图可知，保持运行参数条件相同，若回路中断受阻程度一致，则炉膛中上部稀相区和过渡区同一区域在不同回路中断受阻条件下的颗粒浓度变化规律基本相同。

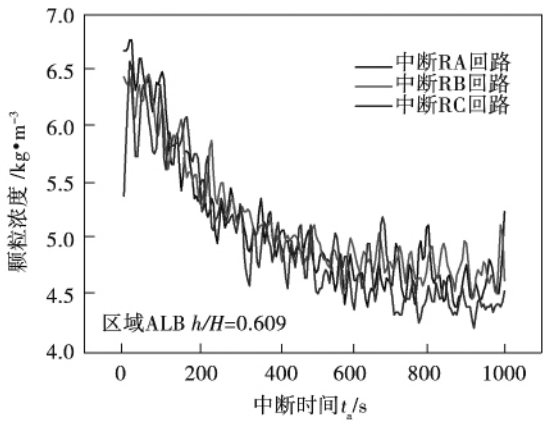

图 7 不同回路中断受阻稀相区（$h/H=0.609$）ALB 区域颗粒浓度变化图

Fig. 7 Chart showing changes of the particle concentration（ALB – $h/H=0.609$） in the sparse phase zone when the loop LB is being interrupted and blocked

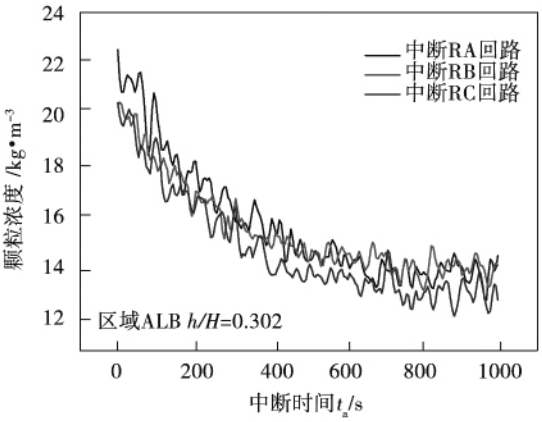

图 8 不同回路中断受阻过渡区（$h/H=0.302$）ALB 区域颗粒浓度变化图

Fig. 8 Chart showing changes of the particle concentration（ALB – h/H = 0.302） in the transition zone when the loop LB is being interrupted and blocked

图 9 给出了炉膛底部密相区的颗粒浓度变化曲线。由图可知，炉膛底部同一区域颗粒浓度变化曲线并不一致：RA 和 RB 回路分别中断受阻时，密相区 ALB 区域颗粒浓度有较明显下降趋势；而 RC 回路中断受阻时，密相区 ALB 区域颗粒浓度基本保持不变。由此可以得出结论：不同的回路中断受阻时，对炉膛底部密相区颗粒浓度的分布产生较大影响，而对炉膛中上部区域颗粒浓度分布影响相对较小。

其原因在于，不同的循环回路中断受阻后，受阻回路回料量减少，从而导致炉膛底部密相区颗粒浓度分布产生较大差异。同时，由于一次风及二次风的强烈扰动作用，炉膛底部密相区颗粒混合扩散剧烈，因而在炉膛中上部区域，固体颗粒浓度分布较为均匀。

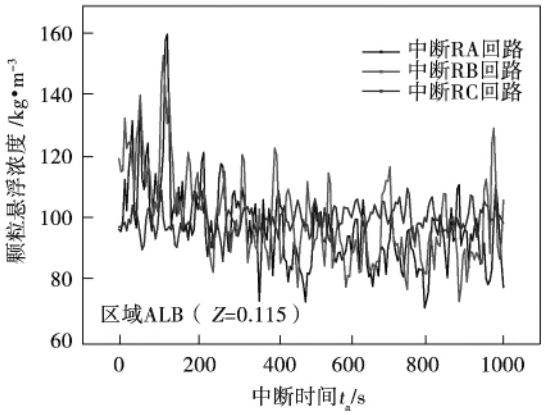

图 9　不同回路中断受阻密相区（$h/H=0.115$）ALB 区域颗粒浓度变化图

Fig. 9 Chart showing changes of the particle concentration(ALB – h/H = 0.115) in the dense phase zone when the loop LB is being interrupted and blocked

3　结　论

本文研究了单回路回料中断受阻时，炉内颗粒浓度的变化规律及不同回路中断受阻对炉内颗粒浓度变化规律的影响，其主要结论如下：

（1）单回路中断受阻后，炉内轴向平均颗粒浓度均成指数型下降，一段时间后装置达至新的平衡状态。恢复回路正常回料后，系统重新恢复到初始平衡状态。

（2）单回路中断受阻后，受炉内强烈气流扰动影响，炉膛中上部横向截面各区域颗粒浓度分布较为均匀。

（3）不同的单回路中断受阻时，炉膛中上部区域颗粒浓度变化规律无明显差异，底部密相区变化规律则较为复杂，系统仍能稳定运行，该性质可为 600 MW 超临界 CFB 锅炉实际运行提供一定的参考。

参考文献：

[1] Hartge E U，Luecke K，Werther J. The role of mixing in the performance of CFB reactors [J]. Chemical Engineering Science，1999(54)：5393 – 5407.

[2] 姜秀民，秦裕琨，刘德昌，等. 油页岩循环流化床燃烧室稀相区流动结构与燃烧特性 [J]. 中国电机工程学报，2001，21(11)：53 – 59.
JIANG Xiu-min，QIN Yu-kun，LIU De-chang，et al. Flow configuration and combustion characteristics of oil shale in the sparse phase zone of a circulating fluidized bed combustor [J]. Proceedings of China Electric Machinery Engineering，2001，21(11)：53 – 59.

[3] Pallar D，Johnsson F. Modeling fuel mixing in a fluidized bed combustor [C]. In 2007 ECI Conference on 12th International Conference on Fluidization-New Horizons in Fluidization Engineering，Vancouver，Canada，2007.

[4] 周　科. 600 MW 循环流化床给煤均匀性实验台架论证与设计 [M]. 武汉：华中科技大学，2008.
ZHOU Ke. Reasoning and design of a coal feed uniformity test rig for 600 MW CFBs [D]. Central China University of Science & Technology，2008.

[5] Zhou，X L，Cheng L M，Wang Q H，et al. Non-uniform distribution of gas-solid flow through six parallel cyclones in a CFB system：An experimental study [J]. Particuology，2012，10(2)：170 – 175.

[6] Blaszczuk，Artur.，Komorowski，et al. Distribution of solids concentration and temperature within combustion chamber of SC-OTU CFB boiler [J]. Journal of Power Technologies，2012，92(1)：27 – 33.

[7] Somjun，Jiraroch，Chinsuwan，et al. Cross sectional suspension density along the height of a CFB riser under fixed and variable bed inventory conditions [J]. Natural Resources and Sustainable Development，2012，3(1)：1882 – 1886.

[8] Wang X Y，Fan B G，Wang S D，et al. Gas-solid flow characteristics in high-density CFB [J]. Journal of Thermal Science，2012，21(4)：354 – 358.

[9] 黄　晨. 大型循环流化床锅炉炉内受热面对流传热特性研究 [D]. 杭州：浙江大学，2012.
HUANG Chen. Investigation of the convective heat transfer characteristics of the heating surfaces in a large-sized circulating fluidized bed boiler [D]. Hangzhou：Zhejiang University，2012.

[10] 周星龙，程乐鸣，张俊春，等. 六回路循环流化床颗粒悬浮浓度及循环流率实验研究 [J]. 中国电机工程学报，2012，32(5)：9 – 14.
ZHOU Xing-long，CHENG Le-ming，ZHANG Jun-chun，et al. Experimental study of the particle suspension concentration and circulating flow rate of a six-loop circulating fluidized bed [J]. Proceedings of China Electric Machinery Engineering，2012，32(5)：9 – 14.

（刘　瑶　编辑）

Montecarlo method, carbon-contained particle, water molecule, adsorption isotherm

大型燃煤火电机组炉前脱硫试验研究 = Experimental Study of the Desulfurization in Front of the Furnace in a Large-sized Coal-fired Thermal Power Generation Unit [刊,汉] /ZHANG Hai-zhen, SONG Hua-wei, HAN Hai-yan, ZHANG Xin (Hua dian Electric Power Research Institute, Hangzhou, China, Post Code: 310030) //Journal of Engineering for Thermal Energy & Power. -2016, 31(11). -64 ~ 68

An experimental study of a large-sized coal-fired thermal power generation unit burning coal with a high sulfur content in the southwest region was performed by using the desulfurization technology in front of the furnace. An on-the-spot test platform was built in a thermal power plant and the sink-float sieving method was used to perform an on-the-spot test of coal ranks with various high sulfur contents commonly used in units. The test results show that to adopt the in-front-of-the-furnace desulfurization technology can effectively lower the sulfur content of coal entering into the furnace and at the meantime can drop the ash content of the coal to a certain extent. The in-front-of-the-furnace desulfurization technology can play an important role in preventing corrosion, reducing the emissions and securing a safe operation of equipment items in coal-fired units and is also significant for large-sized coal-fired units. Only in terms of coal ranks with a high sulfur content chosen, the in-the-front-of-the-furnace desulfurization can force the sulfur content of coal entering into the furnace to averagely lower by about 39.12% and the ash content of the coal to averagely reduce by around 25.01%. **Key words:** large-sized coal-fired thermal power generation unit, desulfurization in front of a furnace, sulfur content, ash content

六回路循环流化床锅炉单回路中断的影响实验研究 = Study of the Influence of the Interruption of a Single Loop on a Six-loop Circulating Fluidized Bed Boiler [刊,汉] /ZOU Yang-jun, HE Sheng (Huadian Electric Power Science Academy, Hangzhou, China, Post Code: 310030), CHENG Le-ming (National Key Laboratory on Energy Source Clean Utilization, Zhejiang University, Hangzhou, China, Post Code: 310027) //Journal of Engineering for Thermal Energy & Power. -2016, 31(11). -69 ~ 73

On a six loop supercritical circulating fluidized bed (CFB) boiler cold-state test rig, the differential pressure method was used to determine the in-furnace particle concentration distribution and study the law governing changes of the in-furnace particle concentration distribution when a single loop is being interrupted and blocked and the influence of the interruption and blockage of various loops on such a law. It has been found that after the single loop has been interrupted and blocked, the axial in-furnace average particle concentration will assume an exponential type decline and renew the initial balance state of the system after the loop has restored its normal material returning, indicating that the "dual-leg" type CFB boiler enjoys self-balancing characteristics. After the single loop has been interrupted and blocked, the particle concentration distribution in various zones in a cross section in the furnace will

be still relatively uniform. When various single loops are being interrupted and blocked, the law governing changes of the particle concentration in the middle and on the top of the furnace will not be significantly different while the law governing changes of the particle concentration in the dense phase zone will be relatively complicated. **Key words:** six loop, circulating fluidized bed, particle condensation, interruption and blockage of a single loop

分布式冷热电联供系统变工况性能实验研究 = Experimental Study of the Off-design Condition Performance of a Distributed Type Cooling, Heating and Power Cogeneration System [刊,汉] /JIANG Run-hua, HUANG Si-min, YIN Hui-bin, YANG Min-lin (Department of Energy and Chemical Engineering, Dongguan University of Technology, Dongguan, China, Post Code: 523808) //Journal of Engineering for Thermal Energy & Power. -2016, 31(11). -74 ~ 79

On the test platform of distributed CCHP systems, off-design performance of units and system has been studied according to the output power of internal combustion engine. The power unit of experimental platform was diesel engine, and the rated power was 50 kW. With the output power of the diesel engine increasing, the primary energy rate (PER) and the relative energy saving ratio (RPESR) are the first to increase and then decrease. When output power is 40 kW, the PER is 76%, and RPESR is 29.5%. When the output power was too low, the RPESR was negative. It means that the CCHP system was not energy saving relative to the production system. The measures to improve the performance of CCHP system have been discussed in this paper. **Key words:** off-design; combined cooling, heating and power system; lithium bromide absorption refrigeration unit; energy utilization ratio

湿式电除尘器充电模型建立与收集效率的数值研究 = Establishment of a Charging Model for Wet Type Electrostatic Precipitators and Numerical Study of the Collection Efficiency [刊,汉] /ZHOU Xiao-ying, CHEN Xiao-ping, DOU Hua-shu (College of Mechanical and Automatic Control, Zhejiang University of Science and Technology, Hangzhou, China, Post Code: 310018), ZHANG Hai-zhen (Huadian Electric Power Science Academy, Hangzhou, China, Post Code: 310030) //Journal of Engineering for Thermal Energy & Power. -2016, 31(11). -80 ~ 86

The finite volume method was used to calculate the particle movement trajectory inside a wet type electrostatic precipitator and the particle collection efficiency of the precipitator. By making use of the test data obtained from the wet type electrostatic precipitator in a 330 MW coal-fired power generation unit, a particle charging model was established and the particle collection efficiency at various circulating water flow rates were analyzed. The Euler multi-phase flow method was employed to calculate a gas-liquid two-phase flow and in combination with a discrete phase model, the ion trajectories were tracked to simulate the three-phase flow inside the precipitator. It has been found that the results calculated by using the numerical calculation model are in relatively good agreement with the